Characterization of surface and nonlinear elasticity in wurtzite ZnO nanowires

Julien Yvonnet, Alexander Mitrushchenkov, Gilberte Chambaud, Qi-Chang He, S.-T. Gu

Characterization of surface and nonlinear elasticity in wurtzite ZnO nanowires

J. Yvonnet,[1, a)] A. Mitrushchenkov,[1] G. Chambaud,[1] Q.-C. He,[1] and S.-T. Gu[2]
[1)] *Université Paris-Est, MSME UMR 8208 CNRS, 5 Bd Descartes 77454 Marne-la-Vallée CEDEX 2, France*
[2)] *Southwest Jiaotong University, School of Mechanical Engineering, Chengdu 610031, PR China*

(Dated: 7 May 2012)

Surface elasticity and nonlinear effects are reported in ZnO nanowires and characterized by *ab initio* calculations. Fully anisotropic elastic and stress coefficients related to $(10\bar{1}0)$ surfaces are provided and used to construct a continuum model of nanowires based on the Gurtin-Murdoch surface elasticity theory, able to capture mechanical size effects. Nonlinear elasticity is observed through non-zero third order energy derivative terms with respect to axial strain in the direction of the nanowire. The associated material parameters are found to be themselves size-dependent.

I. INTRODUCTION

ZnO nanowires have been intensively studied due to their potential in different applications, including electronic and optoelectric devices, gaz sensors, photodetectors[1], integrated nanodevices[2], novel field effect transistors[3,4], detection of polluted or toxic gases and other species[5,6], or prototypes of energy harvesting devices[7,8]. Their unique properties, like quasi-one-dimensionality, wide band gap (3.37 eV), or self assembly[2] make them promising as building blocks for future integrated electronics and mechanical nanosystems. Many ZnO nanostructures can nowadays be routinely synthesized[9–14].

Given the high surface-to-volume ratio of nanowires, effects of surface on their elastic behavior may be prominent, as revealed by the experiment of Chen et al.[15]. The size-dependent mechanical properties can be well explained by the effects of surface energy. In particular, the surface elasticity model provided by Gurtin and Murdoch[16] suits well for characterizing the elastic deformation of nanostructures at the continuum level, as demonstrated experimentally and through simulations[17–20]. That model has been widely adopted to elucidate the surface effects on the elastic bahavior of nanosystems[19–25].

Several first-principles studies have been conducted on wurtzite ZnO surfaces[26–32]. Marana et al.[33] have investigated $(10\bar{1}0)$ and $(11\bar{2}0)$ surfaces by means of DFT, analyzing relaxation and stability, with comparison to experiments. Diebold et al.[34] have studied elastic and acoustic vibrations frequencies with surface effects in ZnO nanoparticles using semi empirical potentials (shell model). Na and Park[35] have analyzed surface energy and surface relaxation of ZnO and ZnS systems by first-principles calculations. Experimental studies on ZnO surfaces can be found e.g. in[36,37]. In all mentioned studies, a simple model for the surface was employed, for example using an isotropic surface stress parameter[38]. Though valid for some systems such as Ag or Pd, this is not the case for ZnO, where the surface behavior is fully anisotropic. It is also worth mentioning that experimental results regarding size effects in ZnO nanowires are highly contradictory, some works reporting an increase of the Young's modulus with a decrease of the diameter[15,39,40], while others[41,42] observe an opposite trend.

The modeling of surface behavior in nanosystems is mandatory to construct continuum models able to operate over a wide range of scales, to avoid restrictions on the number of atoms and to study complex integrated nanosystems. In this work, we characterize surface elasticity, nonlinear effects and their relation to size-dependent effective properties of ZnO wurtzite nanowires, by means of *ab initio* calculations. First, a multiscale continuum model able to take into account arbitrary sizes, geometrical configurations and loads is presented. Then, surface elasticity of ZnO wurtzite nanowires is characterized for $(10\bar{1}0)$ surfaces by identifying constants of the surface elasticity and residual stress tensors. A comparison between the continuum model and full *ab initio* models of nanowires is provided to assess the validity of the multiscale modeling approach. In addition, we report nonlinear elasticity of ZnO nanowires, which is characterized by a non-zero third derivative of the potential energy with respect to axial strain. We show that the corresponding coefficients are also size-dependent.

II. CONTINUUM MODEL

According to the Gurtin-Murdoch model[16], an elastic body defined over a domain $\Omega \in \mathbb{R}^3$, coated by an elastic surface denoted by $\partial\Omega$ is characterized in the absence of body forces by

$$\sigma_{ij,j} = 0 \ \text{ in } \Omega, \tag{1}$$

$$\sigma^s_{kj,i} P_{kj} + [[\sigma_{ij} n_j]] \ \text{ on } \partial\Omega, \tag{2}$$

[a)] Electronic mail: julien.yvonnet@univ-paris-est.fr; http://msme.univ-mlv.fr/staff/meca/yvonnet-julien/.

$$P_{ij} = \delta_{ij} - n_i n_j, \tag{3}$$

$$\sigma_{ij} = C_{ijkl}\varepsilon_{kl}, \tag{4}$$

$$\sigma^s_{ij} = C^s_{ijkl}\varepsilon^s_{kl} + \tau^s_{ij}, \tag{5}$$

where indices correspond to cartesian coordinates, σ and σ^s denote bulk and surface Cauchy stress tensors, $[[.]]$ denotes jump between interface and bulk, P is an orthogonal projector operator describing the projection on the plane tangent to $\partial\Omega$ at $x \in \partial\Omega$ and n is the outward unit normal vector to $\partial\Omega$. In Eqs. (4)-(5), ε and C denote linearized strain and bulk elasticity tensors, and ε^s, C^s and τ^s denote surface strain, surface elasticity, and surface residual stress tensors, respectively. Eq. (1) refers to the bulk equilibrium, Eq. (2) refers to the surface equilibrium[25,43], while Eqs. (4), (5) define the bulk and surface stress-strain constitutive laws. Surface strain is related to bulk counterpart through $\varepsilon^s_{ij} = P_{ik}\varepsilon_{kl}P_{lj}$.

The surface is assumed to be attached to the bulk. Eqs. (1)-(5) are completed by the displacement and traction boundary conditions on respective complementary and disjoint portions of the boundary $\partial\Omega$. The set of equations can be solved numerically for an arbitrary geometry, size, and loading configuration by means of the finite element method[19]. For this purpose, the energy of the system submitted to an applied external force F, in the absence of body forces, expressed by[19,25]

$$\int_\Omega \frac{1}{2}C_{ijkl}\varepsilon_{kl}(u)\varepsilon_{ij}(u)dV + \int_{\partial\Omega}\frac{1}{2}C^s_{ijkl}\varepsilon^s_{kl}(u)\varepsilon^s_{ij}(u)dS = \int_{\partial\Omega} F_i u_i dS - \int_{\partial\Omega}\tau^s_{ij}\varepsilon^s_{ij}(u)dS \tag{6}$$

is varied with respect to the nodal displacements associated to a finite element mesh discretizing the domain Ω. To fully define the problem, the elastic coefficients C_{ijkl}, C^s_{ijkl} and τ^s_{ij} must be characterized. In the case of wurtzite the bulk elastic tensor can be expressed by five independent constants in Voigt's notation: C_{11}, C_{33}, C_{44}, C_{12} and C_{13}. For hexagonal monocrystalline nanowires, the external surfaces are identical and correspond to the $(10\bar{1}0)$ facets. The surface stress can be related to the surface strain through four independent constants C^s_{11}, C^s_{13}, C^s_{33} and C^s_{55} and two residual stress components τ^s_1 and τ^s_3[19,20].

III. IDENTIFICATION OF BULK AND SURFACE ELASTIC PARAMETERS

Elastic parameters are calculated by *ab initio* methods. Computations are performed with the periodic CRYSTAL09 code[44]. This code implements both Hartree-Fock (HF) and Density Functional Theory (DFT) anzats for electronic structure calculations, using Gaussian-type nuclei-centered basis functions to express the electronic wave-functions. In our calculations we use the following basis sets: 86-411d31G for Zn[30] and 8-411(1)G for O[45]. For wurtzite bulk system, both HF and DFT calculations are performed. For DFT, the extra large space integration grid (XXGRID option for CRYSTAL) is employed. The Pack-Monkhorst shrink parameters was set to 8. Both local (PW91, PBESOL) and hybrid (PBE0, B3LYP) DFT functionals have been tested. Note that the hybrid functionals or HF calculations are much more expensive, especially for large slabs or wires with many atoms in the unit cell. Finally, for wires and slabs, PBESOL and PBE0 methods were retained. In CRYSTAL09, the analytic energy derivatives with respect to cell deformation have recently been implemented. This allows for more efficient calculations of elastic constants as first derivatives of code-provided analytic gradients. In our calculations we use the 3-point numerical derivatives with deformation amplitudes of ± 0.005. At all deformed configurations, the nuclear positions were fully relaxed to account for nuclear contribution to elastic properties. The computed values are reported in Table I and compared with experimental data[46]. We note that the different *ab initio* results agree within 5-10% which can thus be considered as a measure of *ab initio* error.

TABLE I. Bulk parameters: units of a, c and u are in Å, while all other elastic constants are in GPa.

	a	c	u	C_{11}	C_{33}	C_{12}	C_{13}	C_{44}
PW91	3.274	5.281	0.379	201.4	216.5	117.6	102.9	34.1
PBESOL	3.237	5.220	0.379	214.9	230.2	133.1	119.4	32.1
PBE0	3.261	5.215	0.381	224.9	229.3	128.5	112.4	41.3
B3LYP	3.281	5.281	0.380	217.2	229.0	116.1	98.8	43.1
HF	3.288	5.232	0.383	241.5	231.9	122.2	102.7	57.7
Expt.[46]	3.250	5.206	0.382	190	196	110	90	39

The same procedure, described in[19,20], is employed for computing the surface parameters. Different slab systems are defined, each comprising a number N of layers with $4N$ atoms in the slab unit cell. In Table II, the elastic parameters of the slab models (in Hartree/atom) are provided with respect to the number of atoms layers N[19,20] using PBE0 and PBESOL functionals, respectively.

To extract surface parameters, these data are fit to a linear function of surface weight

$$w = \frac{2}{N}. \tag{7}$$

For example,

$$C^{slab}_{11}(w) = (1-w)C_{11}(0) + wC^S_{11}, \tag{8}$$

where $C_{11}(0) = C^\infty_{11}$ is a bulk limiting value[19,20]. Figure 1 provides plots of the elastic constants for the slabs with respect to the surface weight w, while figures 2 shows the plots of the surface stress. In these figures, all units

TABLE II. Slab elastic parameters (in Hartree/atom) using PBE0 and PBESOL functionals

N	C_{11}^{slab}	C_{33}^{slab}	C_{13}^{slab}	C_{55}^{slab}	τ_1^{slab}	τ_3^{slab}
PBE0						
3	0.45457	0.38404	0.13944	0.12682	-0.01418	-0.00952
4	0.44783	0.40824	0.13998	0.12359	-0.01032	-0.00679
5	0.44201	0.42391	0.13966	0.12458	-0.00834	-0.00573
6	0.43759	0.43051	0.13767	0.12043	-0.00678	-0.00462
7	0.43475	0.43809	0.13791	0.12083	-0.00590	-0.00421
8	0.43194	0.44137	0.13650	0.11902	-0.00509	-0.00363
9	0.43061	0.44616	0.13689	0.12082	-0.00456	-0.00339
10	0.42862	0.44743	0.13555	0.11803	-0.00402	-0.00296
12	0.42642	0.45345	0.13587	0.11728	-0.00332	-0.00255
20	0.42242	0.46087	0.13439	0.11617	-0.00193	-0.00173
∞	0.41691	0.47641	0.13266	0.11377	0	0
PBESOL						
3	0.38863	0.35218	0.11891	0.09407	-0.01279	-0.00871
4	0.38318	0.37874	0.12230	0.09199	-0.00931	-0.00617
5	0.37825	0.38976	0.12348	0.09075	-0.00741	-0.00465
6	0.37434	0.39867	0.12339	0.09005	-0.00621	-0.00385
7	0.37230	0.40406	0.12282	0.08957	-0.00532	-0.00329
8	0.36968	0.40845	0.12210	0.08920	-0.00466	-0.00285
9	0.36820	0.41191	0.12196	0.08889	-0.00414	-0.00251
10	0.36771	0.41468	0.12219	0.08866	-0.00373	-0.00224
20	0.36159	0.42751	0.12115	0.08727	-0.00190	-0.00121
∞	0.35972	0.44484	0.12349	0.08724	0	0

TABLE III. Surface elastic parameters for ZnO (in N/m).

	C_{11}^s	C_{33}^s	C_{13}^s	C_{55}^s	τ_1^s	τ_3^s
PBE0	49.127	34.899	15.096	13.677	-2.126	-1.362
PBESOL	42.435	32.568	13.345	10.121	-1.906	-1.174

are in Hartree/atom and the PBESOL solution is shown. Conversion from Hartree/atom to N/m is done through

$$C(N/m) = \frac{4}{S} C(Hartree/atom), \tag{9}$$

where $S = ac$ is the area of the surface unit cell.

For coefficient C_{13}^{slab} (see figure 1), the variations of the values with respect to the number of slab layers N are comparable to numerical errors and cannot be used to clearly perform a linear fit. We use only the values for $N \geq 5$ to compute C_{13}^s. It is worth noting that the coefficient C_{13}^s has a negligible influence on the simulation results. The obtained surface elastic parameters are reported in Table III.

IV. COMPARISONS BETWEEN FULL AB INITIO NW MODELS AND CONTINUUM MODEL

To provide a reference solution, full nanowires models with different diameters are solved by *ab initio* calculations. Periodicity is taken into account in the axial direction. Results regarding the effective Young's modulus $\overline{E}$ and axial residual stress $\overline{\tau}_3$ are provided in Table IV

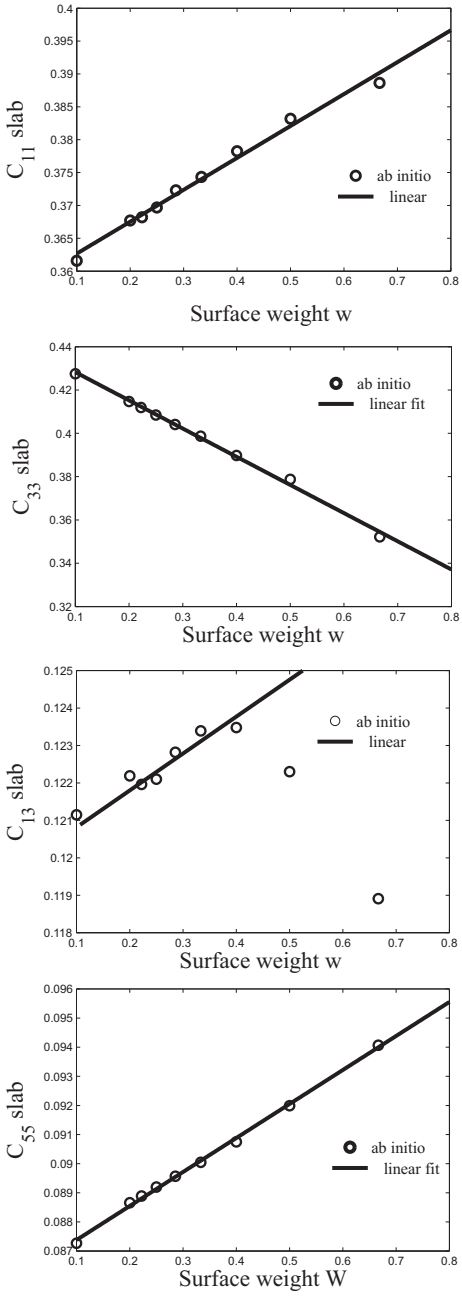

FIG. 1. Sample plots of C_{11}^{slab}, C_{33}^{slab}, C_{13}^{slab} and C_{55}^{slab} against the surface weight w (in Hartree/atom).

in Hartree/atom and in GPa. Conversion into standard units (GPa) is realized by

$$C(GPa) = \frac{M}{V} C(Hartree/atom), \tag{10}$$

where $M = 12N^2$ is the number of atoms in the unit cell, and V is the unit cell volume. The unit cell volume is calculated according to

$$V = \frac{3\sqrt{3}}{8} cd^2, \tag{11}$$

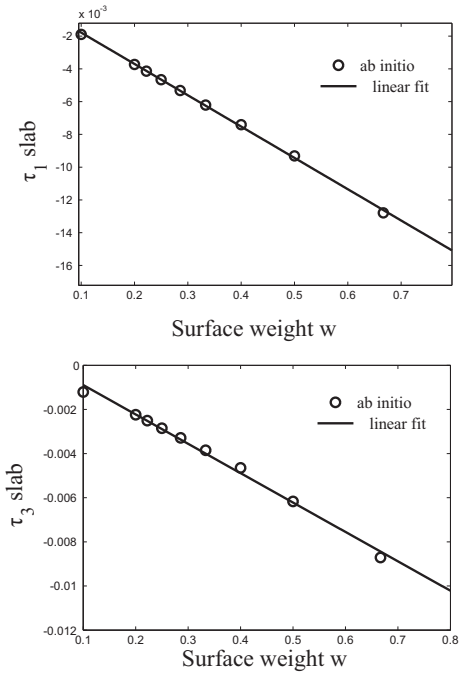

FIG. 2. Sample plots of τ_1^{slab} and τ_3^{slab} against the surface weight w (in Hartree/atom).

where c is the unit cell length (unrelaxed, i.e. taken as the unperturbed bulk value) and d is the nanowire diameter. The definition of the nanowire diameter is controversial. In the present work, we adopt the following definition: we take the unrelaxed nanowire diameter such that the nanowire volume is equal to that of ideal, unrelaxed internal bulk-like part of the nanowire, $V = N_{bulk}\frac{V_{bulk}}{4}$, where $N_{bulk} = 12(N-1)^2$ is the number of atoms in the internal part of the wire, and $\frac{V_{bulk}}{4}$ is the per-atom volume in the bulk material. This definition leads to

$$d = 2(N-1)a. \tag{12}$$

The full *ab initio* results are compared to the solution obtained by solving the finite element model described in[19]. Results related to Young's modulus and axial relaxation $\overline{\varepsilon}_3^0 = -\overline{\tau}/\overline{E}$ are provided in figures 3 (a) and (b). No noticeable change was observed between continuum solutions obtained by both sets of surface elastic parameters reported in table III. In each case, we can note a reasonable agreement between the continuum model using the surface elastic parameters and the full *ab initio* calculations.

V. NONLINEAR EFFECTS

We report nonlinear elasticity when nanowires are stretched in the axial direction. We have computed by *ab initio* method the third derivative of the energy, which is found to be nearly constant with respect to the axial strain. Higher-order derivatives are also computed and found to be negligible. In Hartree/atom, the third derivative of the strain density energy is expressed by

$$T = \frac{1}{M}\frac{\partial^3 E}{\partial \varepsilon_3^3}, \tag{13}$$

with M being the number of atoms per unit cell, and its volume equivalent, in GPa, defined similarly to Young's modulus as

$$T(GPa) = \frac{1}{V}\frac{\partial^3 E}{\partial \varepsilon_3^3}, \tag{14}$$

TABLE IV. Effective elastic Young's modulus $\overline{E}$ and residual stress $\overline{\tau}_3$ (in Hartree/atom) and in GPa

N	$\overline{E}$	$\overline{\tau}_3$	$\overline{E}$	$\overline{\tau}_3$
	PBESOL (in Hartree/atom)		PBE0 (in Hartree/atom)	
2	0.26257	-0.00714	0.28846	-0.00780
3	0.31984	-0.00463	0.33506	-0.00500
4	0.32856	-0.00334	0.35872	-0.00368
5	0.34301	-0.00260	0.37256	-0.00292
6	0.35242	-0.00213	0.38223	-0.00244
7	0.35873	-0.00183	0.39024	-0.00212
∞	0.40245	0	0.43420	0
	PBESOL (in GPa)		PBE0 (in GPa)	
2	386.7	-10.5	419.0	-11.3
3	265.0	-3.84	273.8	-4.09
4	215.1	-2.19	231.6	-2.38
5	197.3	-1.50	211.4	-1.66
6	186.9	-1.13	199.9	-1.28
7	179.8	-0.92	192.9	-1.05
∞	148.3	0	157.8	0

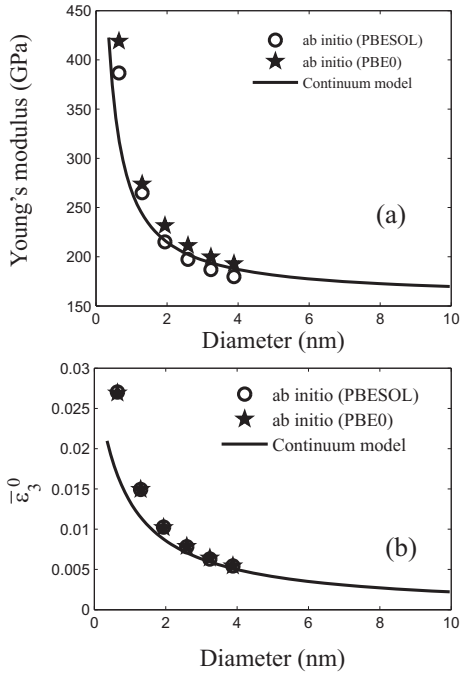

FIG. 3. Comparison between full *ab initio* calculations and continuum model: (a) Young's modulus; (b) axial relaxation strain.

with V being the effective volume of the nanowire defined by Eq.(11). Taking into account this non-linear term, the tangent effective Young's modulus becomes deformation dependent:

$$\overline{E}_T(\varepsilon) = \overline{E} + \varepsilon T. \quad (15)$$

Thus, to get Young's modulus for fully relaxed nanowire, the corresponding value of ε defined in the previous section, must be used. This leads to the predicted value of the relaxed Young's modulus, $\overline{E}_{T,pred} = \overline{E}_T(\overline{\varepsilon}_3^0)$.

The computed values of T are provided in Table V, and the predicted Young's modulus is compared with *ab initio* values $\overline{E}_{T,calc}$ calculated independently at fully relaxed nanowire length. One can immediately notice that accounting for nonlinear term greatly improves the agreement between predicted and calculated values. We further remark that the values of T are size-dependent, when expressed in GPa, while almost constant when expressed in Hartree/atom.

We point out that the change of the reference length in the definition of the strain results in a modified definition of dimensionless deformation and thus in the Young's modulus. We found that this change is very small for the considered cases and can be safely omitted. Also, the unrelaxed diameter was used to calculate both $\overline{E}_{T,pred}$ and $\overline{E}_{T,calc}$. Finally, we point out that if the nonlinearity is taken into account, the continuum model described in section II is no more available. In that case, a full nonlinear constitutive law should be identified for both bulk and surface and an iterative solving procedure should be used to numerically solve the problem.

VI. CONCLUSIONS

We have performed *ab initio* calculations on ZnO $(10\bar{1}0)$ surfaces and on full ZnO nanowires with different diameters. A special procedure has been established to extract the surface elastic coefficients. These coefficients can be used in multiscale continuum models, which are very useful to avoid the limitations of *ab initio* calculations for nanowires of larger diameter, non periodic configurations, or when many interacting nanowires are involved. The conclusions are summarized below.

1. We have provided elastic surface parameters for ZnO wurtzite nanowires using *ab initio* calculations.

2. A continuum model using the computed coefficients has been compared to full ab inito models of wurtzite nanowires. A good agreement is noticed regarding the effective Young's modulus as well as the axial relaxation of the nanowire. The size-dependent properties are well captured by the constructed continuum model.

3. We have reported size-dependent nonlinear elasticity in ZnO nanowires. The related coefficients, also computed by means of *ab initio* calculations, are provided.

ACKNOWLEDGMENTS

The research was supported by the CNRS under grant number 169195.

[1] P. Zhang, F. Xu, A. Navrotsky, J.S. Lee, S.T. Kim and J. Liu, Chem. Mater. 19, 5687 (2009).
[2] Y. Huang, X.F. Duan, Y. Cui, L.J. Lauhon, K.H. Kim and C.M. Lieber, Science. 294, 1313 (2001).
[3] J. Xiang, W. Lu, Y.J. Hu, H. Yan and C.M. Lieber, Nature. 441, 489 (2006).
[4] Y. Cui, H. Zhong, D.L. Wang, W.U. Wang and C.M. Lieber, Nano Lett. 3, 149 (2003).
[5] E. Kanazawa, G. Sakai, Shimanoe, Y. Kanmura, Y. Teraoka, N. Miura and N. Yamazoe, Sens. Actuator B-Chem. 77, 72-77 (2001).
[6] P. Zemva, A. Lesar, I. Kobal and M. Senegacnik, Langmuir. 17, 1543-1548 (2001).
[7] Z.L. Wang, X. Wang, J. Song, J. Liu and Y. Gao, IEEE CS. 7, 49-55 (2008).
[8] W.S. Su, Y.F. Chen, C.L. Hsiao and L.W. Tu, Appl. Phys. Lett. 90, 1-3 (2007).
[9] P. Yang, H. Yan, S. Mao, R. Russo, J. Johnson, R. Saykally, N. Morris, J. Pham, R. He and H.-J. Choi, Adv. Funct. Mater. 12, 323 (2002).
[10] Z.L. Wang, X.Y. Kong, Y. Ding, P. Gao, W.L. Hughes, R. Wang and Y. Zhang, Adv. Funct. Mater. 14, 943 (2004).
[11] C. Wang, C.P. Liu, J.L. Huang, S.-J. Chen, Y.-K. Tseng and S.-C. Kung, Appl. Phys. Lett. 87, 013110 (2005).
[12] W.I. Park, J. Yoo and G.-C. Yi, J. Korean Phys. Soc. 46, L1067 (2005).
[13] K. Xuan, S.L. Ding, Y.R. Yang, Y. Xiao and Z.H. Guo, J. Phys. Soc. Jap. 75, 014711 (2008).
[14] S.-W. Kim , H.-K. Kim, S.-W. Jeong, J.-S. Hur, S. Jang, D. Kim and D. Byun, Sens.J. Korean Phys. Soc. 52, 3033 (2007).
[15] C.Q. Chen, Y. Shi, Y.S. Zhang, J. Zhu and Y.J. Yan, Phys. Rev. Lett. 96, 075505 (2006).
[16] M.E. Gurtin and A.I. Murdoch, Arch. Ration. Mech. Anal. 57, 291 (1975).
[17] R.E. Miller and V.B. Shenoy, Nanotech. 11, 139 (2000).
[18] IJ. He and C.M. Lilley, Nano Lett. 8, 1798 (2008).
[19] J. Yvonnet, A. Mitrushchenkov, G. Chambaud and Q.-C. He, Comput. Meth. Appl. Mech. eng. 200, 614-645 (2011).
[20] A. Mitrushchenkov, G. Chambaud, J. Yvonnet and Q.-C. He, Nanotech. 21, 255702 (2010).
[21] I.H. He, C.W.Lim and B.S.Wu, Int. J. Solids Struct. 41, 847 (2004).
[22] H.L. Duan, J. Wang, Z.P. Huang and B.L. Karihaloo, J. Mech Phys. Solids. 53, 1574 (2005).
[23] G.F. Wang, X.Q. Feng and S.W. Yu, Eur. Phys. Lett. 77, 44002 (2007).
[24] L. Zhu and X.J. Zheng, Euro. Phys. Lett. 83, 66007 (2008).
[25] J. Yvonnet, H. Le Quang and Q.-C. He, Comput. Mech. 42, 704-712 (2008).
[26] A. Wander and N.M. Harrison, Surf. Sci. Lett. 457, L342 (2000).
[27] A. Wander and N.M. Harrison, Surf. Sci. Lett. 468, L851 (2000).
[28] A. Wander, F. Schedin, P. Steadman, A. Norris, R. McGrath, T.S. Turner, G. Thornton and N.M. Harrison, Phys. Rev. Lett. 86, 3811 (2001).
[29] C.B. Duke, R.J. Meyer, A. Paton and P. Mark, Phys. Rev. B. 18, 8 (1978).

TABLE V. Third derivative of energy, T , at bulk c. In parenthesis - at relaxed length. Effect of third derivative at the relaxed Young's modulus (all in GPa). PBE0 functional is used and diameter defined as $d = 2(n-1)a$ for both unrelaxed and relaxed wires.

n	T, $Hartree/atom$	T, GPa	$\overline{E}$	$\overline{E}_{T,pred}$	$\overline{E}_{T,calc}$
2	2.351(-1.338)	3415(-1944)	419.0	511.3	545.0
3	3.282(2.613)	2628(2135)	273.8	313.1	317.7
4	2.894(2.504)	1868(1617)	231.6	250.8	255.2
5	2.897(3.003)	1644(1704)	211.4	224.2	227.4
6	2.824(2.839)	1477(1485)	199.9	209.4	211.1
7	3.155(2.746)	1560(1357)	192.9	201.4	200.7
∞(bulk)	3.40				

[30] J.E. Jaffe, N.M. Harrison and A.C. Hess, Phys. Rev. B 49, 11153 (1994).
[31] P. Schröer, P. Krüger and J. Pollmann, Phys. Rev. B. 49, 24 (2007).
[32] J.M. Carlsson, Comm. Mat. Sci. 22, 24 (2001).
[33] N.L. Marana, V.M. Longo, E. Longo, J.B.L. Martin and J.R. Sambrano, J. Phys. Chem. A. 112, 8958-8963 (2008).
[34] U. Diebold, L.V. Koplit and O. Dulub, Appl. Surf. Sci. 237, 336-342 (2004).
[35] S.-H. Na, C.H. Park, J. Korean Phys. Soc. 54, 867-872 (2009).
[36] O. Dulub, L.A. Boatner and U. Diebold, Surf. Sci. 519, 201 (2002).
[37] F. Ostendorf, S. Torbrügge and M. Reichling, Phys. Rev. B. 77, 041405 (2008).
[38] G. Wang and X. Li, Appl. Phys. Lett. 91, 231912 (2007).
[39] G. Stan, C. V. Ciobanu, P. M. Parthangal, and R. F. Cook, Nano Lett. 7(12), 3691-3697 (2007).
[40] R. Agrawal, B. Peng, E. E. Gdoutos, and H. D. Espinosa, Nano Lett. 8(11), 3668-3674 (2008).
[41] X.D. Bai, P.X. Gao, Z.L. Wang and E.G. Wang, Appl. Phys. Lett. 82, 4806 (2003).
[42] W. Mai and Z.L. Wang, Appl. Phys. Lett. 89, 073112 (2006).
[43] T. Chen, M.-S. Chiu, C.-N. Weng, J. Appl. Phys. 100, 074308 (2006).
[44] R. Dovesi, V.R. Saunders, C. Roetti, R. Orlando, C.M. Zicovich-Wilson, F. Pascale, B. Civalleri, K. Doll, N.M. Harrison, I.J. Bush, Ph. D'Arco and M. Llunell, CRYSTAL06 User's Manual, University of Torino, Torino, (2006).
[45] Lichanot A, Chaillet M., Larrieu C., Dovesi R and Pisani C, Chem. Phys. 164, 383 (1992).
[46] T. Azuhata, M. Takesada, T. Yagi, A. Shikanai, SF. Chichibu et al., J. Appl. Phys. 94, 968 (2003).